Journal of Arid Environments 211 (2023) 104947

Contents lists available at ScienceDirect

Journal of Arid Environments

journal homepage: www.elsevier.com/locate/jaridenv

Assessment of soil CO_2 and NO fluxes in a semi-arid region using machine learning approaches

Morad Mirzaei [a,**], Manouchehr Gorji Anari [a], Eugenio Diaz-Pines [b], Nermina Saronjic [b], Safwan Mohammed [c], Szilard Szabo [d], Seyed Mohammad Nasir Mousavi [e,f], Andrés Caballero-Calvo [g,*]

[a] Department of Soil Science and Engineering, Faculty of Agricultural Engineering and Technology, University of Tehran, Karaj, Iran
[b] Institute of Soil Research, Department of Forest and Soil Sciences, University of Natural Resources and Life Sciences (BOKU), Vienna, Austria
[c] Institute of Land Utilization, Technology and Regional Planning, Faculty of Agricultural and Food Sciences and Environmental Management, University of Debrecen, Debrecen, Hungary
[d] Department of Physical Geography and Geoinformatics, Faculty of Science and Technology, University of Debrecen, Debrecen, 4032, Hungary
[e] Department of Plant, Food, and Environmental Sciences, Faculty of Agriculture, Dalhousie University, Halifax, NS B2N 5E3, Canada
[f] Institute of Land Use, Engineering and Precision Farming Technology, Faculty of Agricultural and Food Sciences and Environmental Management, University of Debrecen, 138 Böszörményi St., 4032, Debrecen, Hungary
[g] Departamento de Análisis Geográfico Regional y Geografía Física, Facultad de Filosofía y Letras, Campus Universitario de Cartuja, University of Granada, 18071, Granada, Spain

ARTICLE INFO

Keywords:
Agroecosystems
Classical regression
Climate change
NO_x
Machine learning
Iran

ABSTRACT

Agricultural lands are sources and sinks of greenhouse gases (GHGs). The identification of the main drivers affecting GHGs is crucial for planning sustainable agronomic practices and mitigating global warming potential. The main aim of this research was to evaluate the impact of environmental drivers (soil temperature and water-filled pore space, WFPS) and crop residue rates on CO_2, NO, and NO_x fluxes under conventional tillage (CT) and no-tillage (NT) systems. The accuracy of Random Forest Regression (RFR), Multiple Adaptive Regression Splines (MARS), and General Linear Models (GLM) in predicting CO_2, NO, and NO_x fluxes were also assessed.

In both CT and NT systems, CO_2, NO, and NO_x fluxes decreased with increasing WFPS. Increasing temperature resulted in higher CO_2 emissions and lower NO and NO_x emissions. Higher residue rates resulted in significant increases in CO_2 emission, whereas the NO and NO_x emissions increased by decreasing the ratio of residue. For CO_2 prediction, the RFR provided the largest R^2 with the observed data. For NO–N and NO_x-N prediction, RFR was the most efficient algorithm, but NO–N can be predicted with better accuracy. The output of this research highlights the importance of agronomic practices for climate mitigation, along with the possibility of using RFR to predict GHGs fluxes.

1. Introduction

Climate change is due to the emissions of greenhouse gases (GHGs) from anthropogenic activities (Smith et al., 2008; IPCC et al., 2019). Carbon dioxide (CO_2) is the major contributor to the increased radiative forcing since the pre-industrial period (WMO, 2020), with major anthropogenic sources of CO_2 including the burning of fossil fuels and deforestation. At the same time, ecosystems, including agroecosystems exchange large amounts of CO_2 with the atmosphere. through the decomposition of soil organic matter and crop, and animal residues (Zechmeister-Boltenstern et al., 2018). The rate of soil CO_2 emissions depends on the land cover, environmental conditions, and soil characteristics (Sugasti and Pinzón, 2020). Agricultural landscapes are also responsible for large N emissions, which occur as ammonia (NH_3), nitric oxide (NO), nitrogen dioxide (NO_2), nitrous oxide (N_2O), and N_2 (Zaman et al., 2012). NO is a secondary greenhouse gas and a key component in the formation of tropospheric ozone (O_3) (Anenberg et al., 2012; Molina-Herrera et al., 2017). Agricultural soils are the main sources of NO emissions (Luo et al., 2012). According to previous studies, the emissions of NO vary from 13 to 27 Tg NO–N a^{-1} (Davidson and Kingerlee,

* Corresponding author.
** Corresponding author.
E-mail addresses: mirzaee.morad1366@yahoo.com (M. Mirzaei), andrescaballero@ugr.es (A. Caballero-Calvo).

https://doi.org/10.1016/j.jaridenv.2023.104947
Received 17 March 2022; Received in revised form 1 January 2023; Accepted 17 January 2023
Available online 20 January 2023
0140-1963/© 2023 The Authors. Published by Elsevier Ltd. This is an open access article under the CC BY-NC-ND license (http://creativecommons.org/licenses/by-nc-nd/4.0/).

1997; Steinkamp and Lawrence, 2011; Hudman et al., 2012). The application of N fertilizers accounts for approximately 60% of soil NO emissions in agriculture (Molina-Herrera et al., 2017). Emissions of NO from agricultural soil occur mainly via nitrification (Rolland et al., 2008; Molina-Herrera et al., 2017), denitrification (Conrad, 2002), and chemo denitrification (Kesik et al., 2005).

Several factors including environmental conditions (e.g. soil moisture, temperature), C/N ratio, and management practices drive the process of GHGs' exchange between the soil and the atmosphere (Medinets et al., 2015; Oertel et al., 2016). Among these factors, soil temperature and soil moisture are used to show a significant effect on the emission of GHGs (Mohammed et al., 2022; Mirzaei et al., 2022a).

Management of the post-harvest crop residue also affects the trace gas fluxes. Estimates indicate that 3.76×10^9 tonnes of crop residue are produced annually worldwide (Lal, 2005). Recent investigations demonstrated that the use of these residues could improve several soil properties and reduce land degradation processes, but more work is still needed to convince farmers and policymakers to financially support them (Rodrigo-Comino et al., 2020; Mirzaei et al., 2021). Changes in crop residue management practices can lead to changes in the soil environment and GHGs emissions (Smith et al., 2007; Mirzaei et al., 2022b, 2023). The effects of crop residue management on GHGs are not conclusive. Changes in GHGs emissions can be due to several factors including the amount of residue, rate of decomposition, added carbon (C) and N, and the effect of these residues on changing soil conditions (Pitombo et al., 2016). Also, soil tillage is one of the most significant agricultural practices affecting GHGs emissions from soil. Conventional tillage (CT) includes primary soil inversion; in contrast, no-tillage (NT) reduces soil disturbance and retains crop residues on the soil surface (Abdalla et al., 2013; Abbas et al., 2020). Previous studies show that CT stimulates the decomposition of organic matter, increases soil respiration, and GHGs emissions (Peterson et al., 2019; Mohammed et al., 2022; Valujeva et al., 2022), while NT reduces soil disturbance and energy consumption, improves the soil quality, increases soil carbon sequestration, and mitigates GHG emissions (Ogle et al., 2019; Mirzaei et al., 2021; Mirzaei et al., 2022a; Bhattacharyya et al., 2022).

Given the raising concerns about increased GHGs emissions from agricultural soils, identification of the impact of environmental and agricultural management practices is crucial for a better understanding of mitigation potential. To disentangle the effect of single parameters (e.g.soil water content, and soil temperature) is usually difficult to address under field conditions, due to the seasonal dynamics, combined with the impact of individual agricultural practices. In this sense, the incubation of soil cores in the laboratory condition is a practical way to overcome these issues (Schaufler et al., 2010) and provide controlled, standardized conditions for a better mechanistic understanding between GHG fluxes and driving parameters. However, to the best of our knowledge, no information is available about laboratory experiments assessing the interactive effects of soil temperature, soil moisture, incorporation of residue rates, and tillage on trace gas fluxes in semi-arid regions.

Machine learning (ML) models algorithms are increasingly used to study environmental phenomena, including GHGs emissions in croplands (Adjuik and Davis, 2022), and have proved useful to select efficient management practices to mitigate the emissions (Saha et al., 2021). . Using pattern recognition, machine learning (ML) explains connections between input and output parameters (Twarakavi et al., 2009; Baker et al., 2018) and generates new options to detect, quantify and understand processes in agriculture (Liakos et al., 2018). However, despite the potential of ML tools, limited studies applied machine learning (ML) algorithms to predict GHGs fluxes from agricultural soil (Tavares et al., 2018; Freitas et al., 2018; Ebrahimi et al., 2019; Hamrani et al., 2020; Saha et al., 2021; Abbasi et al., 2021; Adjuik and Davis, 2022).

We aimed at (i) assessing the effects of temperature, soil moisture, and crop residue rates on soil CO_2, NO, and NOx fluxes under CT and NT systems and (ii) assessing the accuracy of three ML algorithms in predicting soil CO_2, NO, and NOx fluxes. For this, a laboratory incubation with intact soil cores under controlled conditions was conducted.

We hypothesized that: i) the addition of higher residue rates would increase CO_2 emissions and decrease NO fluxes ii) CO_2 and NO fluxes would raise with decreasing the amount of soil water-filled pore space (WFPS).

2. Materials and methods

2.1. Site description and soil sampling

The site under investigation is located at the Agriculture Research Station of the College of Agriculture and Natural Resources, University of Tehran, Karaj, Iran (35°48' 32″ N, 50° 58' 06″ E, 1308 m a.s.l.). It has a semiarid climate with mean air temperature and rainfall of 13.7 °C and 245.5 mm, respectively. Soil samples were collected in July 2019, from two field experiments including conventional tillage (CT) and no-tillage system (NT) systems. Each field was under the application of three rates of crop residues (0, 50, and 100% by weight) from July 2018 to July 2019. More detailed information about the experimental fields can be found in Mirzaei et al. (2021). Intact soil samples (three replicates for each combination of rate of crop residues and of tillage) were collected from the top 5 cm soil depth using Polyvinyl chloride (PVC) cylinders (diameter: 5 cm, height: 5 cm).

2.2. Incubation system and estimation of GHG fluxes

Porosity was estimated using the bulk density for each treatment (1.20 and 1.38 g cm^{-3} for CT and NT, respectively, Mirzaei et al., 2021) and assuming a particle density of 2.65 g cm^{-3}; this calculation yielded a pore percentage of 54.7 and 47.9 for CT and NT respectively, and further served for calculating the total amount of water needed to reach 30, 60 and 90% WFPS. The actual net weight after the soil sampling was used to calculate the actual soil moisture (which was usually between 5 and 20% WFPS) and the missing water was added to each core to reach 30% WFPS. Then, the soils were incubated at 10 °C. After three days, soil samples were weighed and water was added to bring them back to 30 % WFPS (water loss was in the range of 2–3% WFPS); then the soil cores were incubated at 15 °C and the procedure was repeated, before increasing the temperature to 20 °C. Then, the incubator was set at 10 °C again, and soils were watered to reach 60% WFPS; the incubation procedure was repeated (involving 10, 15, and 20 °C); before undergoing a final incubation at 90% WFPS.

We used a fully automated temperature-controlled incubation system, which is a modification from the system described in Schindlbacher et al. (2004) and has been used in several other investigations (e.g. Gritsch et al., 2016; Deltedesco et al., 2019). The system is enclosed in a thermos-cabinet and features adapted jars that act as dynamic chambers (steady-state through-flow chambers (Pumpanen et al., 2004), whereby the exchange rate of gases between the soil and the headspace is estimated by using the concentration difference between the in- and outflow (Butterbach-Bahl et al., 2016).

The gas concentration in the inflow was measured by using an empty, reference chamber. The system can host a total of 22 measurement chambers and two reference ones. The flow rate was set to 1.0 l min^{-1}, which allowed for the stabilization of the outflow concentration within a few minutes. 10 min were required to estimate a flux from a single chamber (4 min for the reading of the reference chamber plus 6 min for the measurement chamber), so that, when fully occupied, the gas fluxes of the 22 cores can be estimated every 4 h. The CO_2 concentrations were estimated with an infrared gas analyser (PP Systems WMA-2, Amesbury, MA, USA). NO and NO_2 concentrations were measured with a chemiluminescence analyzer (HORIBA APNA-360, Kyoto, Japan).

For each combination of temperature and soil moisture (which lasted three days), only the last 4 measurements were used (spanning about 16

h). Due to technical problems, the flux at 60% WFPS was not stored and therefore not available.

2.3. Statistical analysis

We evaluated the factors influencing trace gas fluxes using General Linear Models (GLM). In this case, the GLM was a 3-way factorial ANOVA (residue rates, temperature levels, and WFPS levels). We determined the effect sizes (ω^2p) as a standardized, thus, comparable measure of the magnitude of differences among the factor levels ($\omega^2p >$ 0.14: large, 0.13–0.06: medium, <0.05: small effect). Normal distribution of the residuals was checked with the Shapiro-Wilk test and homoscedasticity with the Levene test (Field et al., 2012), respectively.

2.4. Modeling techniques and prediction strategies

We applied three regression techniques (General Linear Models (GLMs), Random Forest Regression (RFR), and Multiple Adaptive Regression Splines (MARS) to predict the trace gas fluxes as affected by residue rate, temperature, and soil moisture.

Were used. GLMs are the most common multivariate models to predict scale variables against scale or factorial variables. GLMs usually used multiple linear regression with scale-independent variables, but now, we used only factorial (i.e., nominal) variables. We used RFR as an algorithm for regression (prediction of scale values). We applied 500 trees (ntree parameter) as the model error does not increase above 200–300 trees (Boehmke and Greenwell, 2019), but more trees ensure a more robust output. The number of splitting at each tree node (mtry) was determined by the caret package on R, using values of 2, 3, and 5, and considered as 3 for all models. MARS is a robust method for regression that uses an iterative method involving two steps: (i) first, it creates basis functions (BFs) partitioning the range of values of independent variables, models a regression line for each BF and each BF relates to knots, (ii) then, it uses the BFs estimates as predictors, and a least-square model is estimated and pruned (Friedman, 1991). The nprune parameter was determined with 2, 4, and 6 values; finally, 4 was optimal for CO_2, and 2 for NO and NOx models (holding the maximum degree of interaction constant at 1).

For the model evaluation of each technique, we applied 2-fold cross-validation with 25 repetitions. Each dataset was randomly split into a training and a testing subset and then a model was built using the training data; using the model, the testing subset was used to calculate the Pseudo-R^2 (correlation between the observed and predicted values), Mean Absolute Error (MAE) and Root Mean Squared Error (RMSE). Next, the testing subset was used for training a new model, and the previous training subset was used for testing. This procedure was repeated 25 times with new random splits, generating 50 models. Accordingly, all models were evaluated with the medians and interquartile ranges of the 50 repetitions. The most accurate GLM, RFR, and MARS models were determined by using the lowest RMSEs. the caret (Kuhn, 2020); , rpart (Therneau and Atkinson, 2019), and earth (Milborrow, 2020) packages in R 4.04 (R Core Team, 2021) were used.

Predictions were evaluated with the Nash-Sutcliff model efficiency coefficient (NSE) which considers the difference between observed and modelled values and quantifies the difference from the optimal 1:1 line. The NSE values of 1, >0.75, 0.65–0.74, 0.50–0.64, and values of <0.50 can be interpreted as perfect, very good, good, satisfactory, and unsatisfactory respectively (Lufi Suryaningtyas et al., 2020). We also calculated the normalized root mean squared error (NRMSE) values normalized by the maximum-minimum values. Model efficiency on factor level was evaluated by Taylor diagrams that showed the correlation between the observed and modelled data (r), the RMSE of the model, and the standard deviation (SD): the position of a given point provides all this information (Taylor, 2001). NSE and NRMSE were calculated in R 4.04 (R Core Team, 2021) with the hydroGOF package (Zambrano-Bigiarini, 2020) and Taylor diagrams were produced with the openair package (Carslaw and Ropkins, 2012).

3. Results

3.1. Soil CO_2, NO, and NOx fluxes

Emissions of CO_2, NO, and NOx were higher at 30% WFPS than at 90% WFPS. At 30% WFPS, higher temperature resulted in higher CO_2 fluxes but lower NO, and NOx fluxes. At 90% WFPS, no significant differences in fluxes were observed between temperatures. Higher fluxes of CO_2, NO, and NOx were observed across all residue rates in CT compared to NT. The highest fluxes of CO_2 were measured at 30% WFPS and 20 °C. For NO and NOx the highest rates were observed at 30% WFPS and 10 °C which was the first incubation step after the pre-incubation phase (Figs. S1 and S2).

Residue rate, WFPS, and temperature significantly affected the CO_2 emission; furthermore, the interaction of WFPS and temperature was significant (Table 1). Effect sizes (ω^2p) were high for temperature, WFPS (0.30 indicating a large effect), and residue rate (0.23); thus, all three factors had a relevant role in CO_2 emission. The interaction of the WFPS and the temperature had a medium effect (0.109). The interaction of temperature and WFPS on CO_2 emission was also significant in both CT and NT systems. In the CT system, at low WFPS (30%), the rate of CO_2 emission increased with the increasing temperature, and the highest emission (435 mg m^{-2} h^{-1}) was observed at 20 °C, while in 90% WFPS no significant differences were noticed between different temperatures (Fig. S1 A). In the NT system, the emission rate increased with the increasing temperature for both WFPS values (30 and 90%).

NO–N emission was influenced by all three factors ($p < 0.001$, Table 1), and by the interaction between WFPS and temperature. The GLM model explained 74.3% of the variance. The WFPS had the largest effect (0.606), followed by the interaction of WFPS and temperature (0.308). WFPS and residue level had only a small effect ($\omega^2p > 0.06$).

In both CT and NT systems, NO emission decreased significantly with the increasing WFPS. The lowest NO emissions in CT (4 mg m^{-2} h^{-1}) and NT (4 mg m^{-2} h^{-1}), belonged to 90% WFPS (Fig. 1 A, B). With increasing the temperature under both tillage systems, the NO emission rate decreased significantly. At 20 °C, lowest NO emission rate in the CT system (11 μg m^{-2} h^{-1}) and NT (13 μg m^{-2} h^{-1}) was observed (Fig. 1 C, D). In both tillage systems, with the decreasing amount of residues, the NO emission increased and the highest NO emission (53.5 μg m^{-2} h^{-1} for CT and 25.5 μg m^{-2} h^{-1} for NT), was observed in the residue removal treatment (0%), which was also significantly different from the 50 and 100% residue rates (Fig. 1 E, F).

GLM of NOx-N influencing factors explained 65.1% variance (Table 1). WFPS (0.509) and the interaction of WFPS and temperature (0.267) had the highest effects, but the effects of temperature and residue level were also large (0.15). Lower rates of NOx emission were related to the application of higher residue rates treatments, and the highest emission of NO_X was obtained from the residue removal. In the 90% WFPS, the effect of temperature is non-significant (CT) or of low importance (NT). At 30% WFPS, the highest emission rate was observed at 10 °C, and then decreased at 15 and 20 °C (Fig. S1 C). This combination (30% WFPS and 10 °C) was the first incubation condition following the rewetting of dry soils.

3.2. Predicting trace gas fluxes

Regarding the CO_2 prediction, the RFR provided the largest R^2, but it was only 2–3% better than the GLM and the MARS. Similar tendencies were found for MAE, RMSE, NSE, and NRMSE (Table 2, Fig. 2). Similar results were found for NO and NOx fluxes, but RFR performed 8–13% better than the GLM and MARS. Soil NO fluxes could be predicted with better accuracy (64%) than NOx (55%).

Table 1
GLM results of temperature, WFPS, and residue rate on CO_2–C, NO–N, and NOx-N emissions.

Source of variance	df	SS			F			P			ω^2p		
		CO_2–C	NO–N	NOx-N	CO_2–C	NO–N	NOx-N	CO_2–C	NO–N	NOx-N	CO_2–C	NO–N	NOx-N
Model	17	653116	18240	22302	3.69	9.69	6.60	< .001	< .001	< .001	0.47	0.74	0.65
WFPS	1	240145	9224	11264	22.32	80.01	54.70	< .001	< .001	< .001	0.30	0.60	0.50
Temperature	2	219766	2287	2861	10.21	9.92	6.94	< .001	< .001	0.003	0.30	0.28	0.21
Residue rate	2	53336	2053	2086	2.48	8.90	5.06	0.019	< .001	0.012	0.23	0.26	0.15
WFPS × Temperature	2	86496	2684	4039	4.02	11.64	9.80	0.027	< .001	< .001	0.10	0.30	0.26
WFPS × Residue rate	2	4152	603	644	0.19	2.61	1.56	0.825	0.088	0.225	−0.03	0.06	0.02
Temperature × Residue rate	4	35051	391	331	0.81	0.84	0.40	0.525	0.505	0.806	−0.02	0.01	−0.03
WFPS × Temperature × Residue rate	4	14169	997	1078	0.32	2.16	1.30	0.856	0.095	0.287	−0.05	0.08	0.02
Residuals	33	354941	3804	6795									
Total	51	2.48e+6	36882	48529									

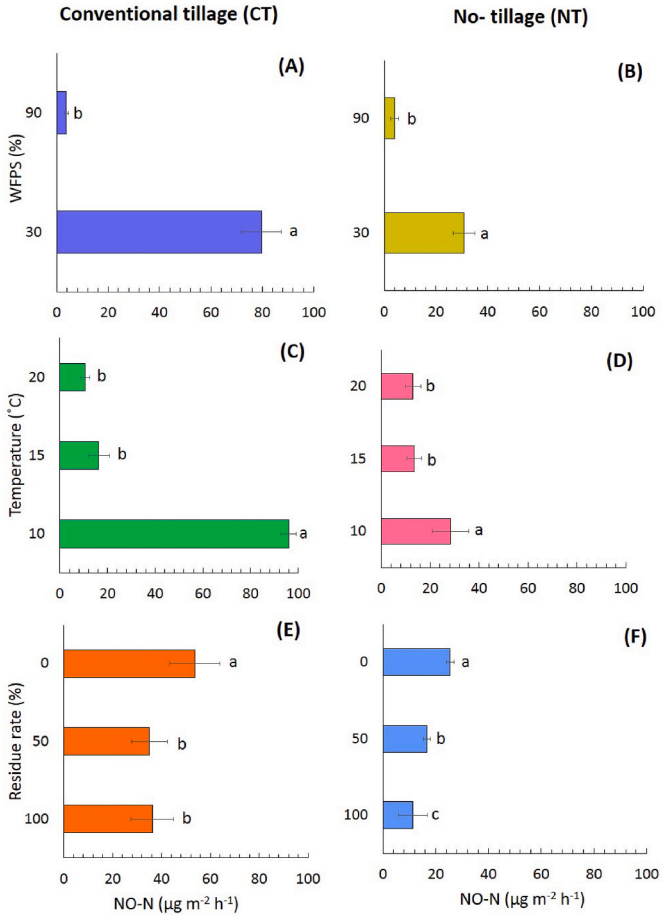

Fig. 1. The effect of soil WFPS (A and B) temperature (C and D), and residue rate (E and F) on NO–N emissions under conventional tillage – CT (left) and no-tillage – NT and (right) systems. Means with the same letter are not significantly different.

3.2.1. *Prediction efficacy by temperature levels*

Considering the temperature levels, we found that RFR was also efficient in predicting CO_2 emissions, both the correlations and the RMSE showed the best fit (Fig. 3A). Although GLM and MARS had similar SDs as the test data at 10 °C, RMSEs were higher. RFR's errors were 8–11 mg m^{-2} h^{-1} smaller than GLM, and 15–37 mg m^{-2} h^{-1} smaller than MARS models. The largest differences were experienced at 15 °C. The average magnitude of error (RMSE) increased with the temperature at all algorithms, in the case of RFR centered errors were 62.4 (10 °C), 75.2 (15 °C), and 94.0 (20 °C).

Regarding the NO–N prediction, correlations were higher than in the case of CO_2; generally, all predictions were more accurate. MARS had the largest relative error (NRMSE, Table 2). RFR's performance was the best at 10 °C with a correlation of r > 0.95 and an RMSE of 12 μg m^{-2} h^{-1} (Fig. 3B). GLM and MARS performed better at 15 and 20 °C, but the overall performance was worse compared to RFR (Table 2). Unlike in the case of CO_2, changes in RMSE did not have a trend: RFR had 12.4, 6.9, and 9.6 at 10-15-20 °C, respectively.

Table 2
Model accuracies (NSE: Nash-Sutcliff coefficient, NRMSE: normalized root mean squared error; GLM: General Linear Model, MARS: Multiple Adaptive Regression Splines, RFR: Random Forest Regression; bold highlight: best model by dependent variables).

Dependent variable	Statistical model	NSE	NRMSE
CO_2	GLM	0.57	18.6
	RFR	**0.66**	**16.6**
	MARS	0.42	21.6
NO–N	GLM	0.65	14.7
	RFR	**0.84**	**9.9**
	MARS	0.4	19.2
NOx-N	GLM	0.6	15.3
	RFR	**0.79**	**11**
	MARS	0.37	19.2

In the case of NOx-N prediction, RFR was the most successful predictor algorithm: RMSE was <14 μg m^{-2} h^{-1}, correlations of modelled and observed values were the highest, and usually higher with 0.09 related to other models (Fig. 3C). GLM's performance was the closest to RFR's accuracy metrics only at 20 °C, RMSE values were 14.6 (RFR) and 14.8 (GLM), but in the other two temperature levels, RFR had 58 and 75% lower RMSE. RMSE did not have a trend, in the case of RFR values were 14.4, 9.1, and 14.6 in the function of increasing temperature.

3.2.2. *Prediction efficacy by residue rates*

The RFR algorithm proved to be a powerful tool in predicting CO_2 emission based on residue rates, compared with MARS and GLM (Fig. 4A). The performance of RFR, MARS, and GLM was almost similar for 50 and 100% residue rates (Fig. 4A). As the results of CO_2 emission prediction, the RFR algorithm was superior to another algorithm in the prediction of NO–N and NO_x-N by residue rates (Fig. 4 B, C). However, for 0 and 100% residue rates the performance of the RFR algorithm was distinguished from the other algorithms. While, for 50% residue rates the performance of the GLM algorithm was almost like RFR (Fig. 4 B, C). In the case of CO_2, RMSR was the lowest at the 0% residue rate (~55), and worse at 50% (~110). For NO–N and NO_x-N, RMSRs were 5–10%, and the 0 and 50% residue rates were the most efficient.

4. Discussion

4.1. *Effects of environmental drivers and agroecosystems management practices CO_2, NO, and NOx fluxes in semiarid regions*

Soil temperature and moisture content are important factors

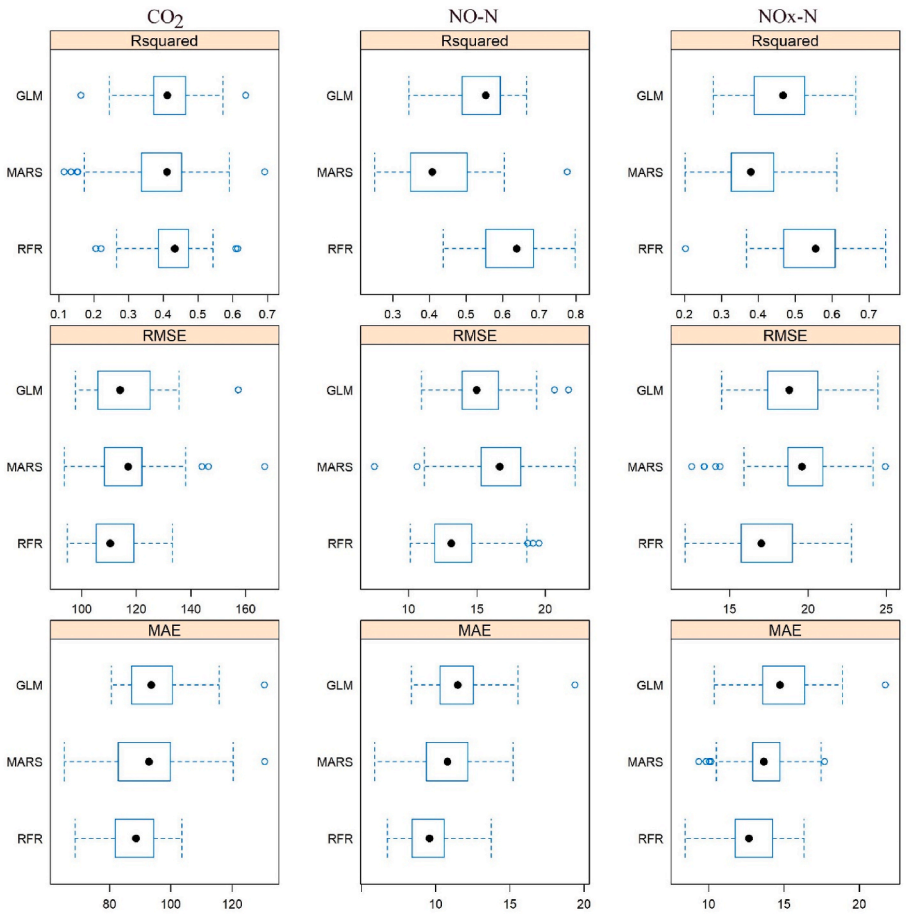

Fig. 2. Classification accuracies of the applied models on CO_2, NO–N, and NOx-N based on 50 models (R^2, RMSE: Root Mean Squared Error, MAE: Mean Absolute Error, GLM: General Linear Model, MARS: Multiple Adaptive Regression Splines, RFR: Random Forest Regression; boxplot shows the minimum, maximum, inter-quartile range, o: outlier, •: median).

controlling microbial processes of N and C transformation and GHGs emissions (Horák et al., 2020). On one hand, a gradual increase in soil temperature will lead to higher microbial activity (Meixner and Yang, 2006); on the other hand, soil water content plays an essential role in supplying substrate for soil microorganisms, and also it determines the availability of oxygen and gas diffusivity (Schindlbacher et al., 2004). Also, temperature increases intensify residue decomposition, providing further carbon precursors for soil microorganisms and ultimately, leading to increased CO_2 emissions (Razavy-Toosi et al., 2017; Wegner et al., 2018). 90% WFPS was probably strongly limiting aeration and, therefore, the diffusivity of air and microbial respiration. However, some other studies (Guo et al., 2012) have reported the maximum CO_2 emissions at 90% WFPS, associated with improved diffusion of available carbon and increased anaerobic respiration, with the latter process probably not being relevant in the climatic context of our experiment. Significant increases in CO_2 emission were noticed in 100 and 50% residue rates treatments compared to residue removal (0%) (Fig. S3 E, F). The significant increase of CO_2 emission in the R_{100} and R_{50} compared to the R_0, which was observed in both CT and NT, can be explained by a substantial input increase from decomposing residue that serves as a substrate for soil microbes (Razavy-Toosi et al., 2017). Crop residue mineralization alters soil organic carbon, microbial biomass, and dissolved organic carbon (Ding et al., 2017; Yang et al., 2017). It has been well documented that most of the added C from residue will respire to the atmosphere (Campos et al., 2011; Mirzaei et al., 2022b).

The highest rates of NO–N and NOx-N fluxes at 10 °C, are mainly attributed to the rewetting effect which happened after pre-incubation. Also under 30% WPFS, higher fluxes of NO–N and NOx-N were recorded compared to 90% WPFS. Increasing soil water saturation raises anaerobic conditions and promotes N_2O emissions via denitrification (Dobbie and Smith, 2001), while NO emissions tend to rise under dryer conditions (Van Dijk and Meixner, 2001; Guckland et al., 2009). In well-aerated soils, NO is produced via nitrification and it is the most emitted gaseous form N from the soil (Russow et al., 2000), while N_2 and N_2O are the main forms of gases N produced in wet soils (Davidson et al., 2000). In agreement with our findings, Schaufler et al. (2010) reported that increasing wetness decrease nitric oxide emissions steadily and the optimum moisture level for NO ranged between 20 and 40% WFPS, with the most increased emissions occurring at 20% WFPS. Also, Del Prado et al. (2006) found that the maximum NO emissions have been recorded below 60% WFPS. In addition, Schindlbacher et al. (2004) found that the optimal moisture for NO emission ranged between 15 and 65% WFPS.

Higher fluxes of NO–N and NOx-N in the residue removal treatment compared to R_{100} and R_{50} could be attributed to the presence of plant residue in R_{100} and R_{50}, which increases moisture content and intensifies microbial activity and thus oxygen consumption, which consequently leads to the creation of small anaerobic conditions (Baggs et al., 2006; Taghizadeh-Toosi et al., 2021) that accelerate the conversion of NO to N_2O and N_2. On the other hand, crop residues affect the dynamics and availability of nitrogen in the soil and the processes of nitrification and denitrification (Schmatz et al., 2020). It is possible that the high C/N ratio of plant residues in R_{100} and R_{50} causes nitrogen immobilization and limits the available nitrogen as an essential factor in NO production. It has been reported that the availability of N is the most important factor for NO emission in the soil (Pilegaard, 2013). In this context, the

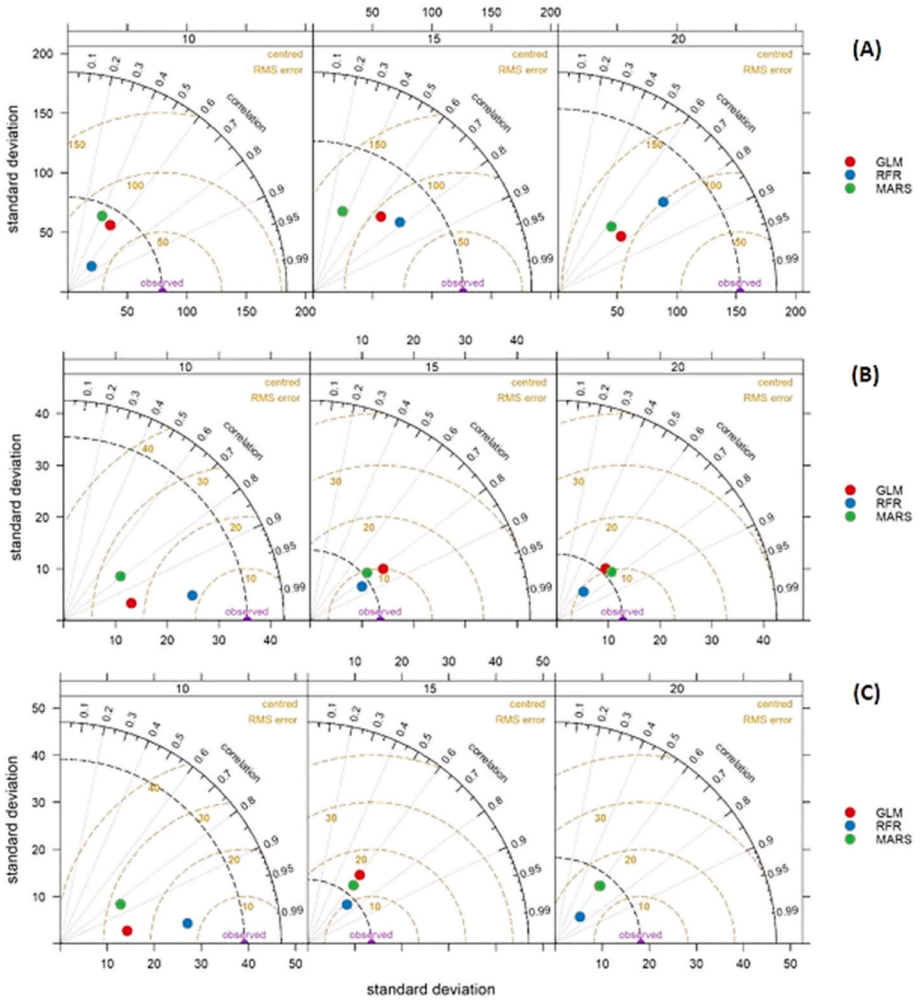

Fig. 3. Model efficacy of CO_2 (A), NO–N (B), and NOx-N (C) predictions by temperature levels (Temp = temperature, °C; GLM: General Linear Model, RFR: Random Forest Regression, MARS: Multiple Adaptive Regression Splines; RMS error: root mean squared error, —: standard deviation of the test data).

C/N ratio is the most important and perhaps the main factor affecting the mineralization and immobilization of nitrogen in the soil which determines the dominant process of nitrogen dynamic in the soil and the decomposition of organic matter (Chen et al., 2014).

4.2. Performance of machine learning algorithm in predicting CO_2, NO, and NOx fluxes in a semiarid region

Recently, ML algorithms have been utilized to investigate complicated environmental phenomena with large temporal and spatial variability (Hamrani et al., 2020; Molnár et al., 2020). In our case, RFR was the most powerful tool in predicting trace gas fluxes, although the difference in performance was not high compared to GLM and MARS. Previously, Hamrani et al. (2020) reported that classical regression models including the RFR have a satisfactory performance in predicting carbon fluxes, with failure in predicting the peak of N_2O fluxes. Similarly, Abbasi et al. (2021) concluded that RFR is a good technique for predicting CO_2 fluxes from the soil regardless of fertilizer level. Furthermore, the RFR algorithm was highlighted as a good tool for the prediction of CO_2 (Shiri et al., 2021) and N_2O fluxes (Saha et al., 2021).

RFR's better performance in predicting GHGs fluxes could be explained by the flexible structure of this algorithm without assumptions on distribution, linearity, or homoscedasticity. The RFR algorithm uses decision trees growing on randomly partitioned subsets with the aim to find the best combination of factors (Abbasi et al., 2021). Compared with the other algorithms (GLM, MARS), the RFR serves as a versatile model that can handle complex interactions and nonlinear relationships among input variables (Abbasi et al., 2021). The ranges of the applied 50 models RFR indicated good reliability (the narrower the interquartile range the more reliable the model, Varga et al., 2021): difference of upper and lower quartile of R^2s were 0.08 for CO_2, 0.13 for NO, and 0.07 for NOx predictions whereas in case of GLM ranges were 0.02–0.04 larger, and the minimums were also worse with 0.04–0,09 units. However, reliability can be increased with a longer period of measurements and involving more sites, which is a task for the future.

5. Conclusions

In this research, we measured the emissions of CO_2, NO, and NOx fluxes from undisturbed soil, obtained from the semiarid region, by using a laboratory incubation technique. Soil samples were obtained from agricultural soils under the application of three different residue rates (100, 50, and 0%) in CT and NT systems. Measurements were conducted under varying conditions of temperature (10, 15, and 20 °C), and soil moisture (30 and 90% WFPS). In the later stage, the observed emissions were used to assess the accuracy of three ML in the prediction of CO_2, NO, and NO_x fluxes. The output of this research can be summarized as follow. CO_2, NO, and NO_x fluxes from cultivated lands were significantly affected by temperature, soil moisture, and residue rate. Interestingly, the interaction between temperature and soil moisture had a significant impact on CO_2 emissions. However, CO_2 emission decreased with the increasing soil moisture. In CT and NT systems, the

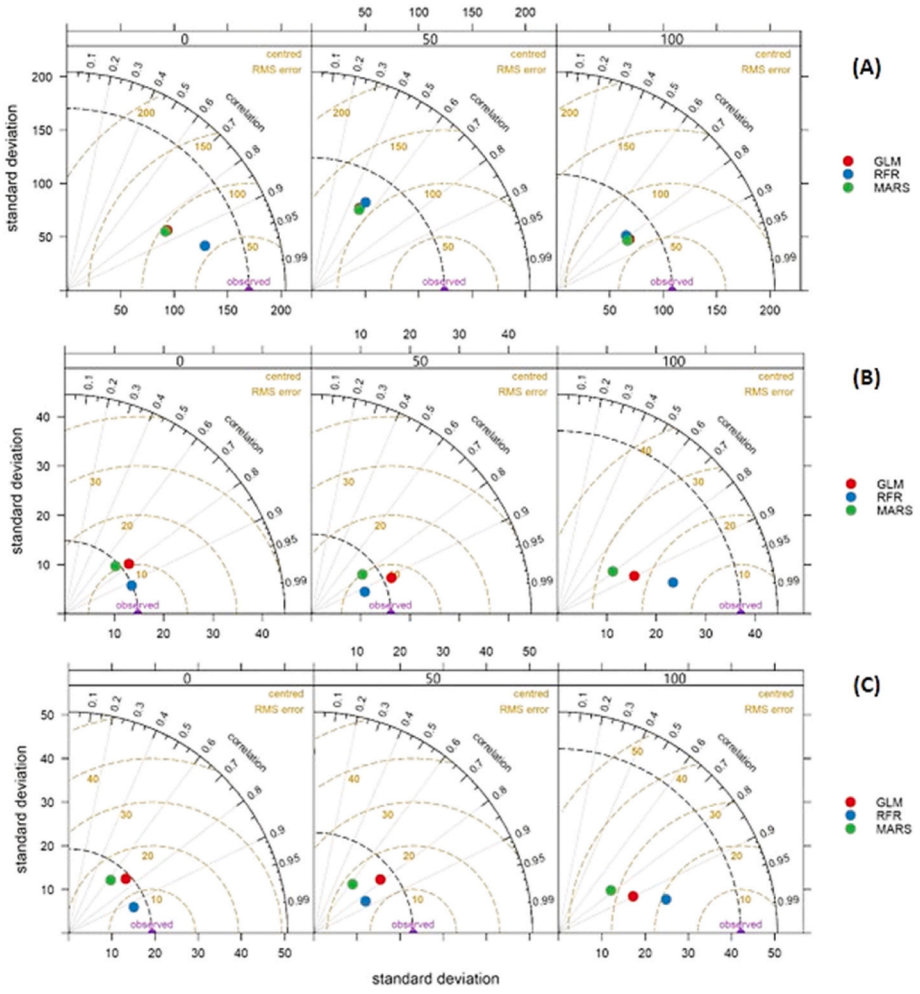

Fig. 4. Model efficacy of CO_2 (A), NO–N (B), and NOx-N (C) predictions by residue rates (GLM: General Linear Model, RFR: Random Forest Regression, MARS: Multiple Adaptive Regression Splines; RMS error: root mean squared error, —: standard deviation of the test data).

NO and NOx emission increased with decreasing rate of residues, the highest NO emission (53.5 μg m^{-2} h^{-1} for CT and 25.5 μg m^{-2} h^{-1} for NT), and NOx emission (56 μg m^{-2} h^{-1} for CT and 27 μg m^{-2} h^{-1} for NT) were observed from the residue removal treatment (0%). Among the three tested ML algorithms (RFR, GLM, MARS), the RFR was the most powerful tool in Predicting CO_2, NO, and NO_x fluxes. Regarding the NO–N prediction, MARS had the largest relative error. However, the RFR's performance was the best at 10 °C. GLM and MARS performed better than RFR at 15 and 20 °C, but the overall performance was worse compared to RFR. The RFR algorithm proved to be a powerful tool in predicting CO_2 emission based on residue rates, compared with MARS and GLM.

Funding

Funding for open access charge: Universidad de Granada/CBUA.

CRediT authorship contribution statement

Morad Mirzaei: Conceptualization, Methodology, Software, Data curation, Writing – original draft, preparation, Writing – review & editing. **Manouchehr Gorji Anari:** Writing – original draft, preparation, Supervision. **Eugenio Diaz-Pines:** Visualization, Investigation, Software, Validation, Writing – review & editing. **Nermina Saronjic:** Methodology, Formal analysis, Validation. **Safwan Mohammed:** Data curation, Software. **Szilard Szabo:** Software, Investigation, Formal analysis. **Seyed Mohammad Nasir Mousavi:** Methodology, Investigation, Formal analysis, Data curation. **Andrés Caballero-Calvo:** Conceptualization, Methodology, Formal analysis, Resources, Writing – original draft, preparation, Writing – review & editing, Validation, Supervision.

Declaration of competing interest

The authors declare that they have no known competing financial interests or personal relationships that could have appeared to influence the work reported in this paper.

Data availability

Data will be made available on request.

Acknowledgments

Szilard Szabo was supported by the TKP2021-NKTA-32 (NKFI). Safwan Mohammed was supported by the project no. TKP2021-NKTA-32 with the support provided by the National Research, Development, and Innovation Fund of Hungary, financed under the TKP2021-NKTA funding scheme.

Appendix A. Supplementary data

Supplementary data to this article can be found online at https://doi.org/10.1016/j.jaridenv.2023.104947.

References

Abbasi, N.A., Hamrani, A., Madramootoo, C.A., Zhang, T., Tan, C.S., Goyal, M.K., 2021. Modelling carbon dioxide emissions under a maize-soy rotation using machine learning. Biosyst. Eng. 212, 1–18.

Abbas, F., Hammad, H.M., Ishaq, W., Farooque, A.A., Bakhat, H.F., Zia, Z., et al., 2020. A review of soil carbon dynamics resulting from agricultural practices. J. Environ. Manag. 268, 110319.

Abdalla, M., Osborne, B., Lanigan, G., Forristal, D., Williams, M., Smith, P., Jones, M.B., 2013. Conservation tillage systems: a review of its consequences for greenhouse gas emissions. Soil Use Manag. 29 (2), 199–209.

Adjuik, T.A., Davis, S.C., 2022. Machine learning approach to simulate soil CO_2 fluxes under cropping systems. Agronomy 12 (1), 197.

Anenberg, S.C., Schwartz, J., Shindell, D., Amann, M., Faluvegi, G., Klimont, Z., JanssensMaenhout, G., Pozzoli, L., Van Dingenen, R., Vignati, E., 2012. Global air quality and health co-benefits of mitigating near-term climate change through methane andblack carbon emission controls. Environ. Health Perspect. 120, 831–839.

Baggs, E.M., Chebii, J., Ndufa, J.K., 2006. A short-term investigation of trace gas emissions following tillage and no-tillage of agroforestry residues in western Kenya. Soil Tillage Res. 90 (1–2), 69–76.

Baker, R.E., Pena, J.M., Jayamohan, J., Jérusalem, A., 2018. Mechanistic models versus machine learning, a fight worth fighting for the biological community? Biol. Lett. 14 (5), 20170660.

Bhattacharyya, S.S., Leite, F.F.G.D., France, C.L., Adekoya, A.O., Ros, G.H., de Vries, W., Melchor-Martínez, E.M., Iqbal, H.M., Parra-Saldívar, R., 2022. Soil Carbon Sequestration, Greenhouse Gas Emissions, and Water Pollution under Different Tillage Practices. Science of the Total Environment, 154161.

Boehmke, B., Greenwell, B., 2019. Hands-on Machine Learning with R. Chapman and Hall/CRC.

Butterbach-Bahl, K., Sander, B.O., Pelster, D., Díaz-Pinés, E., 2016. Quantifying greenhouse gas emissions from managed and natural soils. In: Rosenstock, T.S., Rufino, M.C., Butterbach-Bahl, K., Wollenberg, L., Richards, M. (Eds.), Methods for Measuring Greenhouse Gas Balances and Evaluating Mitigation Options in Smallholder Agriculture. Springer International Publishing, Cham, pp. 71–96.

Campos, B.H.C.D., Amado, T.J.C., Tornquist, C.G., Nicoloso, R.D.S., Fiorin, J.E., 2011. Long-term C-CO_2 emissions and carbon crop residue mineralization in an oxisol under different tillage and crop rotation systems. Rev. Bras. Ciência do Solo 35 (3), 819–832.

Carslaw, D.C., Ropkins, K., 2012. Openair—an R package for air quality data analysis. Environ. Model. Software 27, 52–61.

Chen, B., Liu, E., Tian, Q., Yan, C., Zhang, Y., 2014. Soil nitrogen dynamics and crop residues. A review. Agronomy Sustain. Develop. 34 (2), 429–442.

Conrad, R., 2002. Microbiological and biochemical background of production and consumption of NO and N2O in soil. In: Gasche, R., Papen, H., Rennenberg, H. (Eds.), Trace Gas Exchange in Forest Ecosystems, vol. 3. Springer, Netherlands.

Davidson, E.A., Keller, M., Erickson, H.E., Verchot, L.V., Veldkamp, E., 2000. Testing a conceptual model of soil emissions of nitrous and nitric oxides. Bioscience 50, 667–680.

Davidson, E., Kingerlee, W., 1997. A global inventory of nitric oxide emissions from soils. Nutrient Cycl. Agroecosyst. 48, 37–50. https://doi.org/10.1023/a: 1009738715891.

Del Prado, A., Merino, P., Estavillo, J.M., Pinto, M., Gonzales-Murua, C., 2006. N2O and NO emissions from different N sources and under a range of soil water contents. Nutrient Cycl. Agroecosyst. 74, 229–243.

Deltedesco, E., Keiblinger, K.M., Naynar, M., Piepho, H.P., Gorfer, M., Herndl, M., et al., 2019. Trace gas fluxes from managed grassland soil subject to multifactorial climate change manipulation. Appl. Soil Ecol. 137, 1–11.

Ding, R., Wang, W., Zhang, Q., 2017. Effect of straw mulching on soil respiration and its' temperature sensitivity under different crop rotation systems. Chin. J. Eco-Agric. 25 (8), 1106–1118.

Dobbie, K.E., Smith, K.A., 2001. The effects of temperature, water-filled pore space and land use on N_2O emissions from an imperfectly drained gleysol. Eur. J. Soil Sci. 52, 667–673.

Ebrahimi, M., Sarikhani, M.R., Sinegani, A.A.S., Ahmadi, A., Keesstra, S., 2019. Estimating the soil respiration under different land uses using artificial neural network and linear regression models. Catena 174, 371–382.

Field, A., Miles, J., Field, Z., 2012. Discovering Statistics Using R. Sage publications.

Freitas, L.P., Lopes, M.L., Carvalho, L.B., Panosso, A.R., La Scala Júnior, N., Freitas, R.L., et al., 2018. Forecasting the spatiotemporal variability of soil CO2 emissions in sugarcane areas in southeastern Brazil using artificial neural networks. Environ. Monit. Assess. 190 (12), 1–14.

Friedman, J.H., 1991. Multivariate adaptive regression splines. Ann. Stat. 1–67.

Gritsch, C., Egger, F., Zehetner, F., Zechmeister-Boltenstern, S., 2016. The effect of temperature and moisture on trace gas emissions from deciduous and coniferous leaf litter. J. Geophys. Res.: Biogeosciences 121 (5), 1339–1351.

Guckland, A., Flessa, H., Prenzel, J., 2009. Controls of temporal and spatial variability of methane uptake in soils of a temperate deciduous forest with different abundance of European beech (Fagus sylvatica L.). Soil Biol. Biochem. 41, 1659–1667.

Guo, X., Drury, C.F., Yang, X., Reynolds, W.D., Zhang, R., 2012. Impacts of wet–dry cycles and a range of constant water contents on carbon mineralization in soils under three cropping treatments. Soil Sci. Soc. Am. J. 76 (2), 485–493.

Hamrani, A., Akbarzadeh, A., Madramootoo, C.A., 2020. Machine learning for predicting greenhouse gas emissions from agricultural soils. Sci. Total Environ. 741, 140338.

Horák, J., Igaz, D., Aydin, E., Šimanský, V., Buchkina, N., Balashov, E., 2020. Changes in direct CO_2 and N_2O emissions from a loam Haplic Luvisol under conventional moldboard and reduced tillage during growing season and post-harvest period of red clover. J. Hydrol. Hydromechanics 68 (3), 271–278.

Hudman, R.C., Moore, N.E., Mebust, A.K., Martin, R.V., Russell, A.R., Valin, L.C., Cohen, R.C., 2012. Steps towards a mechanistic model of global soil nitric oxide emissions: implementation and space based-constraints. Atmos. Chem. Phys. 12, 7779–7795. https://doi.org/10.5194/acp-12-7779-2012.

IPCC, 2019. Summary for policymakers. In: Shukla, P.R., Skea, J., Calvo Buendia, E., Masson-Delmotte, V., Pörtner, H.-O., Roberts, D.C., Zhai, P., Slade, R., Connors, S., van Diemen, R., Ferrat, M., Haughey, E., Luz, S., Neogi, S., Pathak, M., Petzold, J., Portugal Pereira, J., Vyas, P., Huntley, E., Kissick, K., Belkacemi, M., Malley, J. (Eds.), Climate Change and Land: an IPCC Special Report on Climate Change, Desertification, Land Degradation, Sustainable Land Management, Food Security, and Greenhouse Gas Fluxes in Terrestrial Ecosystems (in press).

Kesik, M., Ambus, P., Baritz, R., Bruggemann, N.B., Butterbach-Bahl, K., Damm, M., Duyzer, J., Horvath, L., Kiese, R., Kitzler, B., Leip, A., Li, C., Pihlatie, M., Pilegaard, K., Seufert, G., Simpson, D., Skiba, U., Smiatek, G., Vesala, T., Zechmeister-Boltenstern, S., 2005. Inventories of N_2O and NO emissions from European forest soils. Biogeosciences 2, 353–375. https://doi.org/10.5194/bg-2-353-2005.

Kuhn, M., 2020. Classification and Regression Training [R Package Caret Version 6.0-86. Comprehensive R Archive Network (CRAN).

Lal, R., 2005. World crop residues production and implications of its use as a biofuel. Environ. Int. 31, 575–584. https://doi.org/10.1016/j.envint.2004.09.005.

Liakos, K.G., Busato, P., Moshou, D., Pearson, S., Bochtis, D., 2018. Machine learning in agriculture: a review. Sensors 18 (8), 2674.

Lufi Suryaningtyas, S., Ery, S., Rispiningtati, R., 2020. Hydrological analysis of TRMM (Tropical rainfall measuring mission) data in Lesti sub watershed. Civil Environ. Sci. J. (Civense) 3 (1), 18–30.

Luo, G.J., Brueggemann, N., Wolf, B., Gasche, R., Grote, R., Butterbach-Bahl, K., 2012. Decadal variability of soil CO_2, NO, N_2O, and CH4 fluxes at the Hoglwald Forest, Germany. Biogeosciences 9, 1741–1763. https://doi.org/10.5194/bg-9-1741- 2012.

Meixner, F.X., Yang, W.X., 2006. Biogenic emissions of nitric oxide and nitrous oxide from arid and semi-arid land. In: Dryland Ecohydrology. Springer, Dordrecht, pp. 233–255.

Medinets, S., Skiba, U., Rennenberg, H., Butterbach-Bahl, K., 2015. A review of soil NO transformation: associated processes and possible physiological significance on organisms. Soil Biol. Biochem. 80, 92–117.

Milborrow, S., 2020. Derived from Mda: Mars by Trevor Hastie and Rob Tibshirani. Uses Alan Miller's Fortran Utilities with Thomas Lumley's Leaps Wrapper. Earth: Multivariate Adaptive Regression Splines Version 5.1. 2. CRAN from.

Mirzaei, M., Gorji Anari, M., Razavy-Toosi, E., Asadi, H., Moghiseh, E., Saronjic, N., Rodrigo-Comino, J., 2021. Preliminary effects of crop residue management on soil quality and crop production under different soil management regimes in corn-wheat rotation systems. Agronomy 11 (2), 302.

Mirzaei, M., Anari, M.G., Razavy-Toosi, E., Zaman, M., Saronjic, N., Zamir, S.M., et al., 2022a. Crop residues in corn-wheat rotation in a semi-arid region increase CO_2 efflux under conventional tillage but not in a no-tillage system. Pedobiologia 93, 150819.

Mirzaei, M., Gorji Anari, M., Taghizadeh-Toosi, A., Zaman, M., Saronjic, N., Mohammed, S., et al., 2022b. Soil nitrous oxide emissions following crop residues management in corn-wheat rotation under conventional and No-tillage systems. Air Soil. Water Res. 15, 11786221221128789.

Mirzaei, M., Gorji Anari, M., Saronjic, N., Sarkar, S., Kral, I., Gronauer, A., Mohammed, S., Caballero-Calvo, A., 2023. Environmental impacts of corn silage production: influence of wheat residues under contrasting tillage management types. Environ. Monit. Assess. 195 (1), 1–20.

Mohammed, S., Mirzaei, M., Pappné Törő, Á., Anari, M.G., Moghiseh, E., Asadi, H., et al., 2022. Soil carbon dioxide emissions from maize (Zea mays L.) fields as influenced by tillage management and climate. Irrigat. Drain. 71 (1), 228–240.

Molina-Herrera, S., Haas, E., Grote, R., Kiese, R., Klatt, S., Kraus, D., et al., 2017. Importance of soil NO emissions for the total atmospheric NOx budget of Saxony, Germany. Atmos. Environ. 152, 61–76.

Molnár, V.É., Simon, E., Ninsawat, S., Tóthmérész, B., Szabó, S., 2020. Pollution assessment based on element concentration of tree Leaves and Topsoil in Ayutthaya Province, Thailand. Int. J. Environ. Res. Publ. Health 17 (14), 5165.

Oertel, C., Matschullat, J., Zurba, K., Zimmermann, F., Erasmi, S., 2016. Greenhouse gas emissions from soils—a review. Geochemistry 76 (3), 327–352.

Ogle, S.M., Alsaker, C., Baldock, J., Bernoux, M., Breidt, F.J., McConkey, B., et al., 2019. Climate and soil characteristics determine where no-till management can store carbon in soils and mitigate greenhouse gas emissions. Sci. Rep. 9 (1), 1–8.

Peterson, B.L., Hanna, L., Steiner, J.L., 2019. Reduced soil disturbance: Positive effects on greenhouse gas efflux and soil N losses in winter wheat systems of the southern plains. Soil Tillage Res. 191, 317–326.

Pilegaard, K., 2013. Processes regulating nitric oxide emissions from soils. Philos. Trans. R. Soc. B 368. https://doi.org/10.1098/rstb.2013.0126.

Pitombo, L.M., do Carmo, J.B., De Hollander, M., Rossetto, R., López, M.V., Cantarella, H., Kuramae, E.E., 2016. Exploring soil microbial 16S rRNA sequence data to increase carbon yield and nitrogen efficiency of a bioenergy crop. Global Change Biology Bioenergy 8 (5), 867–879.

Pumpanen, J., Kolari, P., Ilvesniemi, H., Minkkinen, K., Vesala, T., Niinistö, S., Lohila, A., Larmola, T., Morero, M., Pihlatie, M., Janssens, I., Yuste, J.C., Grünzweig, J.M., Reth, S., Subke, J.-A., Savage, K., Kutsch, W., Østreng, G., Ziegler, W., Anthoni, P., Lindroth, A., Hari, P., 2004. Comparison of different chamber techniques for measuring soil CO_2 efflux. Agric. For. Meteorol. 123, 159–176.

Razavy-Toosi, E., Kravchenko, A.N., Guber, A.K., Rivers, M.L., 2017. Pore characteristics regulate priming and fate of carbon from plant residue. Soil Biol. Biochem. 113, 219–230.

Rodrigo-Comino, J., Giménez-Morera, A., Panagos, P., Pourghasemi, H.R., Pulido, M., Cerdà, A., 2020. The potential of straw mulch as a nature-based solution for soil erosion in olive plantation treated with glyphosate: a biophysical and socioeconomic assessment. Land Degrad. Dev. 31, 1877–1889. https://doi.org/10.1002/ldr.3305.

Rolland, M.N., Gabrielle, B., Laville, P., Serça, D., Cortinovis, J., Larmanou, E., et al., 2008. Modeling of nitric oxide emissions from temperate agricultural soils. Nutrient Cycl. Agroecosyst. 80 (1), 75–93.

Russow, R., Sich, I., Neue, H.U., 2000. The formation of the trace gases NO and N2O in soils by the coupled processes of nitrification and denitrification: results of kinetic 15N tracer investigations. Chemosphere 2, 359–366.

Saha, D., Basso, B., Robertson, G.P., 2021. Machine learning improves predictions of agricultural nitrous oxide (N_2O) emissions from intensively managed cropping systems. Environ. Res. Lett. 16 (2), 024004.

Schaufler, G., Kitzler, B., Schindlbacher, A., Skiba, U., Sutton, M.A., Zechmeister-Boltenstern, S., 2010. Greenhouse gas emissions from European soils under different land use: effects of soil moisture and temperature. Eur. J. Soil Sci. 61 (5), 683–696.

Schindlbacher, A., Zechmeister-Boltenstern, S., Butterbach-Bahl, K., 2004. Effects of soil moisture and temperature on NO, NO_2, and N_2O emissions from European forest soils. J. Geophys. Res. Atmos. 109 (D17302).

Schmatz, R., Recous, S., Weiler, D.A., Pilecco, G.E., Schu, A.L., Giovelli, R.L., Giacomini, S.J., 2020. How the mass and quality of wheat and vetch mulches affect drivers of soil N_2O emissions. Geoderma 372, 114395.

Shiri, N., Shiri, J., Kazemi, M.H., Xu, T., 2021. Estimation of CO2 flux components over northern hemisphere forest ecosystems by using random forest method through temporal and spatial data scanning procedures. Environ. Sci. Pollut. Control Ser. 1–15.

Smith, P., Martino, D., Cai, Z., Gwary, D., Janzen, H., Kumar, P., et al., 2008. Greenhouse gas mitigation in agriculture. Phil. Trans. Biol. Sci. 363 (1492), 789–813.

Smith, P., Martino, D., Cai, Z., Gwary, D., Janzen, H., Kumar, P., et al., 2007. Policy and technological constraints to implementation of greenhouse gas mitigation options in agriculture. Agric. Ecosyst. Environ. 118 (1–4), 6–28.

Steinkamp, J., Lawrence, M.G., 2011. Improvement and evaluation of simulated global biogenic soil NO emissions in an AC-GCM. Atmos. Chem. Phys. 11, 6063–6082. https://doi.org/10.5194/acp-11-6063-2011.

Sugasti, L., Pinzón, R., 2020. First approach of Abiotic drivers of soil CO2 efflux in Barro Colorado Island, Panama. Air Soil. Water Res. 13, 1178622120960096 https://doi.org/10.1177/1178622120960096.

Taghizadeh-Toosi, A., Janz, B., Labouriau, R., Olesen, J.E., Butterbach-Bahl, K., Petersen, S.O., 2021. Nitrous oxide emissions from red clover and winter wheat residues depend on interacting effects of distribution, soil N availability and moisture level. Plant Soil 1–18.

Tavares, R.L.M., Oliveira, S.R.D.M., Barros, F.M.M.D., Farhate, C.V.V., Souza, Z.M.D., Scala Junior, N.L., 2018. Prediction of soil CO 2 flux in sugarcane management systems using the random forest approach. Sci. Agric. 75, 281–287.

Taylor, K.E., 2001. Summarizing multiple aspects of model performance in a single diagram. J. Geophys. Res. Atmos. 106 (D7), 7183–7192.

Therneau, T., Atkinson, B., 2019. Rpart: Recursive Partitioning and Regression Trees. R Package Version 4, pp. 1–15, 2019.

Twarakavi, N.K., Šimůnek, J., Schaap, M.G., 2009. Development of pedotransfer functions for estimation of soil hydraulic parameters using support vector machines. Soil Sci. Soc. Am. J. 73 (5), 1443–1452.

Valujeva, K., Pilecka-Ulcugaceva, J., Skiste, O., Liepa, S., Lagzdins, A., Grinfelde, I., 2022. Soil tillage and agricultural crops affect greenhouse gas emissions from Cambic Calcisol in a temperate climate. Acta Agric. Scand. Sect. B Soil Plant Sci 72 (1), 835–846.

Van Dijk, S.M., Meixner, F.X., 2001. Production and consumption of NO in forest and pasture soils from the Amazon Basin. Water Air Soil Pollut. Focus 1, 119–130.

Varga, O.G., Kovács, Z., Bekő, L., Burai, P., Csatáriné Szabó, Z., Holb, I., et al., 2021. Validation of visually interpreted corine land cover classes with spectral values of satellite images and machine learning. Rem. Sens. 13 (5), 857.

Wegner, B.R., Chalise, K.S., Singh, S., Lai, L., Abagandura, G.O., Kumar, S., et al., 2018. Response of soil surface greenhouse gas fluxes to crop residue removal and cover crops under a corn–soybean rotation. J. Environ. Qual. 47 (5), 1146–1154.

WMO, 2020. The state of greenhouse gases in the atmosphere based on global observations through 2019. WMO Greenhouse Gas Bulletin 16, 1–8.

Yang, X., Meng, J., Lan, Y., Chen, W., Yang, T., Yuan, J., Liu, S., Han, J., 2017. Effects of maize stover and its biochar on soil CO_2 emissions and labile organic carbon fractions in northeast China. Agric. Ecosyst. Environ. 240, 24–31.

Zaman, M., Nguyen, M.L., Šimek, M., Nawaz, S., Khan, M.J., Babar, M.N., Zaman, S., 2012. Emissions of Nitrous Oxide (N_2O) and Di-nitrogen (N_2) from the Agricultural Landscapes, Sources, Sinks, and Factors Affecting N_2O and N_2 Ratios. IntechOpen, pp. 3–32.

Zambrano-Bigiarini, M., 2020. Package 'hydroGOF'. Goodness-Of-Fit Functions for Comparison of Simulated and Observed Hydrological Time.

Zechmeister-Boltenstern, S., Díaz-Pinés, E., Spann, C., Hofmann, K., Schnecker, J., Reinsch, S., 2018. Soil—the hidden Part of climate: microbial processes regulating soil–atmosphere exchange of greenhouse gases. In: Soil and Climate. CRC Press, pp. 11–60.